

# Dirac–Maxwell Solitons

C. Sean Bohun<sup>1)</sup> and F. I. Cooperstock<sup>2)</sup>

1) *Department of Mathematics and Statistics, University of Victoria,  
P.O. Box 3045, Victoria, B.C., Canada V8W 3P4*

2) *Department of Physics and Astronomy, University of Victoria,  
P.O. Box 3055, Victoria, B.C., Canada V8W 3P6*

## ABSTRACT

Detailed analysis of the coupled Dirac–Maxwell equations and the structure of their solutions is presented. Numerical solutions of the field equations in the case of spherical symmetry with negligible gravitational self-interaction reveal the existence of families of solitons with electric field dominance that are completely determined by the observed charge and mass of the underlying particles. A soliton is found which has the charge and mass of the electron as well as a charge radius of  $10^{-23}m$ . This is well within the present experimentally determined upper limit of  $\simeq 10^{-18}m$ . Properties of these particles as well as possible extension to the work herein are discussed.

1999 PACS numbers: 03.65.Ge, 11.10.Lm, 12.20.Ds

## 1 Introduction

Through the years, a number of authors have attempted to avoid the problems inherent in the point-particle model by focussing upon finite soliton-like structures. Fields interacting non-linearly provide the binding without invoking any phenomenological elements. Einstein and Rosen[1] pointed out many years ago that particles should be contained within a field theory and not exist as independent entities. Rosen[2] made considerable progress in implementing such a program in a gauge-invariant manner by minimally coupling a scalar field to the Maxwell field. However, the soliton solutions yielded negative masses. Later[3], neutral quantized particle states of positive mass were found and a more complicated model invoking up to three scalar fields coupled to the Maxwell field was shown to be capable of modeling the known massive leptons[4]. However, the particles were spinless and the view then was that a subsequent quantization of the theory would induce spin.

In 1991, one of the present authors[5] suggested an alternative route to elementary particle modelling, namely as solitons of Dirac–Maxwell theory. Since Dirac–Maxwell theory had been so successful in describing electron spin and magnetic moment, predicting the existence of the positron and refining the energy levels in interacting systems such as hydrogen, it

seemed reasonable that this might successfully extend to a self-interacting soliton structure to model the elementary particles themselves. Spin would already exist in such a model via the spinor structure of the wave function. Shortly thereafter, such solitons were found and their properties studied[6]. A few years later, Lisi[7] independently discovered some of the results in[6]. Recently, there has been a revival of interest in this field and in particular, the issue of gravitational coupling in the Dirac–Maxwell system has been considered[8]. However, there was the misconception that gravitation was a necessary ingredient for the creation of the soliton.

In this paper, we develop the essential results in[5] and[6] and discuss the role of gravitation in soliton structure. The experimental inputs are the respective masses of the electron, muon and tau, their charge and as a constraint, the upper limit to their size which is  $\simeq 10^{-16}$  cm. The plan of the paper is as follows: in sec. 2, we set out the essential coupled Dirac–Maxwell equations to be solved. The structure of the Dirac wave function in spherical coordinates is given and particularized to the case of electric field dominance. The equation is separated in sec. 3 and we contrast the standard treatment in which a potential function is imposed such as in the case of hydrogen and the present case of the soliton where the derivation of the potential is part of the problem. The formal structure of the potential in terms of the Green’s function is given. It is shown that there do exist spherically symmetric potentials for appropriate choices of quantum numbers.

In sec. 4, the spherically symmetric energy-momentum tensor is derived. The relationship between the parameters in the Dirac equation and the physically measured quantities is discussed and the expression for the spatial spread of the soliton is given. The various constraints including singularity avoidance lead to the required boundary conditions for the problem.

In sec. 5, the results are presented. New variables of convenience for numerical integration are introduced. The parameters leading to twenty ground state solitons are listed. It is found that there is a critical range which leads to solitons within the experimentally observed upper limit to the size of the electron. Excited states are presented and the mass ratios are found.

In the final section 6, the essential achievements as well as the limitations of the results are discussed. It is stressed that the solitons have been found without the requirement of significant gravitational interaction and it is conjectured that gravity will be significant for Dirac–Maxwell solitons when  $e/m \simeq 1$  in units for which  $G = c = 1$ . In cgs units, this is  $2.58 \times 10^{-4}$  esugm $^{-1}$ . By contrast, the  $e/m$  ratio for the electron is  $2.04 \times 10^{21}$  or  $5.27 \times 10^{17}$  esugm $^{-1}$  in cgs units.

## 2 Derivation of the Equations

The field equations are obtained from the Lagrangian of quantum electrodynamics[9]

$$L = i\hbar c \bar{\psi} \gamma^\mu \partial_\mu \psi - mc^2 \bar{\psi} \psi - \frac{1}{16\pi} F^{\mu\nu} F_{\mu\nu} - e \bar{\psi} \gamma^\mu \psi A_\mu \quad (1)$$

where  $\psi = (\psi_1, \psi_2, \psi_3, \psi_4)^T$  is the Dirac spinor,  $\bar{\psi} = \psi^\dagger \gamma^0 = (\psi_1^*, \psi_2^*, -\psi_3^*, -\psi_4^*)$ ,  $A^\mu = (\varphi, \mathbf{A})$  is the electromagnetic four-vector potential and  $F^{\mu\nu} = \partial^\mu A^\nu - \partial^\nu A^\mu$  is the Maxwell tensor. The  $\gamma^\mu$  are  $4 \times 4$  Hermitian anticommuting matrices of the unit square

$$\gamma^0 = \begin{pmatrix} I & 0 \\ 0 & -I \end{pmatrix}, \quad \gamma^k = \begin{pmatrix} 0 & \sigma_k \\ -\sigma_k & 0 \end{pmatrix}, \quad k = 1, 2, 3$$

where  $I$  is the unit  $2 \times 2$  matrix and the  $\sigma_k$  are the Pauli matrices

$$\sigma_1 = \begin{pmatrix} 0 & 1 \\ 1 & 0 \end{pmatrix}, \quad \sigma_2 = \begin{pmatrix} 0 & -i \\ i & 0 \end{pmatrix}, \quad \sigma_3 = \begin{pmatrix} 1 & 0 \\ 0 & -1 \end{pmatrix}.$$

Variation with respect to  $A_\mu$  and  $\bar{\psi}$  respectively, yield the field equations

$$F^{\mu\nu}{}_{,\nu} = -4\pi \bar{\psi} \gamma^\mu \psi \quad (2)$$

$$i\hbar c \gamma^\mu \partial_\mu \psi - mc^2 \psi - e \gamma^\mu \psi A_\mu = 0. \quad (3)$$

If  $\psi$  is chosen to be an energy eigenstate with energy  $E$  and one chooses a static charge distribution with a four-vector potential of the form

$$A^\mu = (\phi(r, \theta, \varphi), \mathbf{A}^k(r, \theta, \varphi)), \quad k = 1, 2, 3$$

then the equations (2)-(3) are reduced to

$$\left[ -i\hbar c \boldsymbol{\alpha} \cdot \boldsymbol{\nabla} + \alpha_4 mc^2 - e \boldsymbol{\alpha} \cdot \mathbf{A} + e\phi - E \right] \psi = 0 \quad (4)$$

$$\nabla^2 \phi = -4\pi e \psi^\dagger \psi \quad (5)$$

$$\boldsymbol{\nabla} \times (\boldsymbol{\nabla} \times \mathbf{A}) = 4\pi e \psi^\dagger \boldsymbol{\alpha} \psi \quad (6)$$

where  $\alpha^k = \gamma^0 \gamma^k$ .

In spherical coordinates,  $(x, y, z) = (r \sin \theta \cos \varphi, r \sin \theta \sin \varphi, r \cos \theta)$ , the Dirac wave function has the structure[10]

$$\psi(r, \theta, \varphi) = \begin{pmatrix} \sqrt{\frac{l-m}{2l+1}} g Y_l^m \\ \sqrt{\frac{l+m+1}{2l+1}} g Y_l^{m+1} \\ -i \sqrt{\frac{l+m}{2l-1}} f Y_{l-1}^m \\ i \sqrt{\frac{l-m-1}{2l-1}} f Y_{l-1}^{m+1} \end{pmatrix}_{[j=l+1/2]}, \quad \psi(r, \theta, \varphi) = \begin{pmatrix} \sqrt{\frac{l+m+1}{2l+1}} g Y_l^m \\ -\sqrt{\frac{l-m}{2l+1}} g Y_l^{m+1} \\ -i \sqrt{\frac{l-m+1}{2l+3}} f Y_{l+1}^m \\ -i \sqrt{\frac{l+m+2}{2l+3}} f Y_{l+1}^{m+1} \end{pmatrix}_{[j=l-1/2]} \quad (7)$$

where  $f = f(r)$ ,  $g = g(r)$  and the  $\{Y_l^m(\theta, \varphi)\}_{l,m}$  is the set of orthonormal spherical harmonics defined for  $l = 0, 1, \dots$ ,  $m = -l, -l + 1, \dots, l$  and

$$Y_l^m(\theta, \varphi) = \sqrt{\frac{2l+1}{4\pi} \frac{(l-m)!}{(l+m)!}} P_l^m(\cos \theta) e^{im\varphi}. \quad (8)$$

In addition,  $m$  is an integer such that  $-j \leq m + 1/2 \leq j$ ;  $(m + 1/2)\hbar$  is the  $z$ -component of the total angular momentum.

Consider the spinor with  $j = 1/2$ ,  $l = 0$  and  $m = 0$  which implies from the above representation (7)

$$\begin{aligned} 4\pi\psi^\dagger\psi &= f(r)^2 + g(r)^2 \\ 4\pi\psi^\dagger\boldsymbol{\alpha}\psi &= 2f(r)g(r) \sin \theta (-\sin \varphi, \cos \varphi, 0)^T. \end{aligned}$$

Resolving equations (5) and (6) into spherical coordinates gives

$$\begin{aligned} \nabla^2\phi &= -e \left( f(r)^2 + g(r)^2 \right) \\ \nabla \times (\nabla \times \mathbf{A}) \Big|_{\hat{r}} &= 0 \\ \nabla \times (\nabla \times \mathbf{A}) \Big|_{\hat{\theta}} &= 0 \\ \nabla \times (\nabla \times \mathbf{A}) \Big|_{\hat{\varphi}} &= 2ef(r)g(r) \sin \theta. \end{aligned}$$

Therefore, a four-vector potential of the form

$$A^\mu = (\phi(r), -A_\varphi(r, \theta) \sin \varphi, A_\varphi(r, \theta) \cos \varphi, 0)$$

should be chosen where the components satisfy

$$\frac{d^2\phi}{dr^2} + \frac{2}{r} \frac{d\phi}{dr} = -e \left( f(r)^2 + g(r)^2 \right) \quad (9)$$

$$\frac{\partial^2 A_\varphi}{\partial r^2} + \frac{2}{r} \frac{\partial A_\varphi}{\partial r} + \frac{\cot \theta}{r^2} \frac{\partial A_\varphi}{\partial \theta} + \frac{1}{r^2} \frac{\partial^2 A_\varphi}{\partial \theta^2} - \frac{A_\varphi}{r^2 \sin^2 \theta} = -2ef(r)g(r) \sin \theta. \quad (10)$$

Since the right hand side of equation (10) is nonzero, the theory can only be exact if  $A_\varphi$  is nonzero. However at this point we will impose the assumption of electric field dominance and hence the dominance of  $\phi$  over  $\mathbf{A}$  or  $f(r)$  dominance over  $g(r)$ .

For the validity of the approximation  $\mathbf{A} = \mathbf{0}$ , one radial component of the spinor must dominate over the other so that

$$fg \ll f^2 + g^2.$$

It will be demonstrated that such objects do exist within the non-linear field. With this approximation the equations to solve reduce to a Dirac equation coupled to a Poisson equation:

$$\left[ -i\hbar\boldsymbol{\alpha} \cdot \nabla + \alpha_4 mc^2 + V(r) \right] \psi = E\psi \quad (11)$$

$$\nabla^2 V = -4\pi e^2 \psi^\dagger \psi. \quad (12)$$

With these facts in mind, we now turn to the separation of the stationary Dirac equation (11) with respect to a general central potential and the derivation of the form of  $\psi^\dagger \psi$  for a general set of quantum numbers.

### 3 Separation of the Equation

The separation procedure follows that given in Bethe and Salpeter[10]. First one introduces quantum numbers  $l$  and  $j$ ;  $l$  is the orbital angular momentum quantum number as well as being an integer  $\geq 0$ ;  $j$  is the total angular momentum quantum number and can assume just the two values  $l + 1/2$  and  $l - 1/2$ , (but only  $+1/2$  for  $l = 0$ ). The forms assumed by the four components of  $\psi$  are given explicitly in (7).

The explicit form of the Dirac equation (11) for the four components of the wave function is:

$$\frac{\partial \psi_3}{\partial z} + \frac{\partial \psi_4}{\partial x} - i \frac{\partial \psi_4}{\partial y} - \frac{i}{\hbar c} [E - V(r) - mc^2] \psi_1 = 0 \quad (13)$$

$$\frac{\partial \psi_4}{\partial z} - \frac{\partial \psi_3}{\partial x} - i \frac{\partial \psi_3}{\partial y} + \frac{i}{\hbar c} [E - V(r) - mc^2] \psi_2 = 0 \quad (14)$$

$$\frac{\partial \psi_1}{\partial z} + \frac{\partial \psi_2}{\partial x} - i \frac{\partial \psi_2}{\partial y} - \frac{i}{\hbar c} [E - V(r) + mc^2] \psi_3 = 0 \quad (15)$$

$$\frac{\partial \psi_2}{\partial z} - \frac{\partial \psi_1}{\partial x} - i \frac{\partial \psi_1}{\partial y} + \frac{i}{\hbar c} [E - V(r) + mc^2] \psi_4 = 0. \quad (16)$$

Therefore, by inserting the assumed wave functions (7) into (13)-(16) and using identities similar to (A.6) we find that the following two coupled equations between  $f$  and  $g$  hold:

$$\frac{1}{\hbar c} [E - V(r) + mc^2] f(r) - \left[ \frac{dg}{dr} + \frac{1 + \kappa}{r} g(r) \right] = 0 \quad (17)$$

$$\frac{1}{\hbar c} [E - V(r) - mc^2] g(r) + \left[ \frac{df}{dr} + \frac{1 - \kappa}{r} f(r) \right] = 0 \quad (18)$$

where the new quantum number  $\kappa$  is defined as

$$\kappa = \begin{cases} -l - 1 & \text{for } j = l + 1/2 \quad (l = 0, 1, \dots) \\ l & \text{for } j = l - 1/2 \quad (l = 1, 2, \dots). \end{cases} \quad (19)$$

These equations are valid for all spherically symmetric potentials  $V(\mathbf{r}) = V(r)$  and together they replace expression (11).

At this point, the standard procedure is to specify an external spherically symmetric potential, an example of which is the electrostatic potential energy of the proton-electron

interaction. That is, simply

$$V(r) = -\frac{Ze^2}{r},$$

which is the fundamental solution of Laplace's equation[11]

$$\nabla^2 V = 4\pi Ze^2 \delta^3(\mathbf{r}) \quad (20)$$

where  $\delta^3(\mathbf{r})$  is a three dimensional Dirac delta function centered at the origin. This is consistent with the far range<sup>1</sup> behaviour that we expect to find for the self-field of the fermion since, when we compare (20) with (12) we see that the fermion is treated as an object without structure through the equality,

$$\psi^\dagger \psi = -\delta^3(\mathbf{r}).$$

There is one additional problem that must be explored, namely how to couple relation (5) to (17)-(18). This will be achieved in three parts. First, we find the Green's function for the equation (5). Second, we find an analytic form for the probability density  $\psi^\dagger \psi$  using (7). Once this equation is known, we can proceed to the third step which is to find  $V(r)$  by forming the convolution of the Green's function of step one, with the probability density of step two.

The potential  $V(r)$  satisfies the Poisson equation (12) and by assuming that the solution is sufficiently regular, this can be converted to an integral equation[12]

$$V(\mathbf{r}) = -4\pi e^2 \int G(\mathbf{r}, \mathbf{r}') \psi^\dagger(\mathbf{r}') \psi(\mathbf{r}') d\mathbf{r}' \quad (21)$$

where  $G(\mathbf{r}, \mathbf{r}')$  is the Green's function of the Laplacian operator in three dimensions

$$G(\mathbf{r}, \mathbf{r}') = -\frac{1}{4\pi} \frac{1}{|\mathbf{r} - \mathbf{r}'|} = -\sum_{l=0}^{\infty} \frac{1}{2l+1} \frac{r_{<}^l}{r_{>}^{l+1}} \sum_{m=-l}^l Y_l^m(\theta, \varphi) Y_l^{m*}(\theta', \varphi'). \quad (22)$$

With the Green's function determined, we can turn our attention to the probability density. This is accomplished by using a pair of identities for the associated Legendre functions<sup>2</sup>

$$(1 - \mu^2) \left( P_l^{m+1} \right)^2 = \left[ (l - m) \mu P_l^m - (l + m) P_{l-1}^m \right]^2, \quad (23)$$

$$(1 - \mu^2) \left( P_{l-1}^{m+1} \right)^2 = \left[ (l + m) \mu P_{l-1}^m - (l - m) P_l^m \right]^2 \quad (24)$$

together with the definition of the spherical harmonics (8). The resulting expression for the charge density of the Dirac particle is given by

$$\psi^\dagger \psi = \frac{f^2 + g^2}{2l+1} \left[ (l - m) |Y_l^{m+1}|^2 + (l + m + 1) |Y_l^m|^2 \right] \quad (25)$$

<sup>1</sup>By far range, we mean those distances much larger than the Bohr radius  $r \gg \hbar^2/me^2$ .

<sup>2</sup>Both Eqs. (23)-(24) follow directly from Eqs. (8.5.1) and (8.5.3) of Abramowitz & Stegun[13].

when  $j = l + 1/2$  and

$$\psi^\dagger \psi = \frac{f^2 + g^2}{2l + 1} \left[ (l + m + 1) |Y_l^{m+1}|^2 + (l - m) |Y_l^m|^2 \right] \quad (26)$$

when  $j = l - 1/2$ .

Therefore by using (21), (22) and (25), one obtains the expression

$$\begin{aligned} V(\mathbf{r}) &= -4\pi e^2 \int G(\mathbf{r}, \mathbf{r}') \psi^\dagger(\mathbf{r}') \psi(\mathbf{r}') d\mathbf{r}' \\ &= \frac{4\pi e^2}{2l' + 1} \int \sum_{l=0}^{\infty} \frac{r_{<}^l}{r_{>}^{l+1}} \sum_{m=-l}^l \frac{1}{2l + 1} Y_l^m(\theta, \varphi) Y_l^m(\theta', \varphi') \left[ f(r')^2 + g(r')^2 \right] \\ &\quad \times \left[ (l' - m') |Y_{l'}^{m'+1}(\theta', \varphi')|^2 + (l' + m' + 1) |Y_{l'}^{m'}(\theta', \varphi')|^2 \right] r'^2 dr' d(\cos \theta') d\varphi' \end{aligned}$$

for the case  $j = l + 1/2$ . Similarly, with the use of (26), it can be shown that the potential  $V(\mathbf{r})$  takes the form

$$\begin{aligned} V(\mathbf{r}) &= \frac{4\pi e^2}{2l' + 1} \int \sum_{l=0}^{\infty} \frac{r_{<}^l}{r_{>}^{l+1}} \sum_{m=-l}^l \frac{1}{2l + 1} Y_l^m(\theta, \varphi) Y_l^m(\theta', \varphi') \left[ f(r')^2 + g(r')^2 \right] \\ &\quad \times \left[ (l' + m' + 1) |Y_{l'}^{m'+1}(\theta', \varphi')|^2 + (l' - m') |Y_{l'}^{m'}(\theta', \varphi')|^2 \right] r'^2 dr' d(\cos \theta') d\varphi' \end{aligned}$$

for the case  $j = l - 1/2$ . It is to be noted that the primed indices ( $l', m'$ ) correspond to the angular momentum of the particle, while the unprimed indices run over the complete set of permissible angular momentum quantum numbers. By performing the angular integration of the above formulae, one can immediately conclude that both of the above integrals vanish except when  $m = 0$  and  $l = 0, 2, \dots, 2l'$ . This implies that

$$\begin{aligned} V(\mathbf{r}) &= 4\pi e^2 \frac{2(l' - j')}{2l' + 1} \sum_{n=0}^{l'} \frac{Y_{2n}^0(\theta, \varphi)}{4n + 1} \int_{r'=0}^{\infty} \frac{r_{<}^{2n}}{r_{>}^{2n+1}} \left[ f(r')^2 + g(r')^2 \right] r'^2 dr' \\ &\quad \times \left[ (\kappa' + m' + 1) \langle l', m' + 1 | Y_{2n}^0 | l', m' + 1 \rangle + (\kappa' - m') \langle l', m' | Y_{2n}^0 | l', m' \rangle \right] \quad (27) \end{aligned}$$

where the cases  $j = l \pm 1/2$  have been combined by the application of the definition of  $\kappa'$ . Expression (27) replaces the equation (12). When written in this form, it is clearly seen that the potential  $V(\mathbf{r})$  is not in general spherically symmetric. Table 1 lists the potential (27) for  $l' = 0, 1$  and illustrates the fact that there exists spherically symmetric states with  $l' \neq 0$ .

A localized solution of this model must satisfy the field equations (17) and (18) for  $f$  and  $g$  and a given energy  $E$  where the potential is given by the expression (27). Moreover, it is required that the total probability

$$\langle \psi | \psi \rangle = \sum_{i=1}^4 \langle \psi_i | \psi_i \rangle = \int_0^\infty (f^2 + g^2) r^2 dr < \infty.$$

Since the equations which describe the spatial evolution of the wave function (17)-(18) were derived under the assumption that the potential,  $V(r)$ , is spherically symmetric, they are not valid for an extended Dirac particle in an arbitrary state of angular momentum. We have shown that there do exist certain choices of  $l$  and  $m$  where the probability density is spherically symmetric and it is these cases in which our primary interest lies.

We can conclude that with the spinor representation given by (7), there are essentially three differential equations to be solved simultaneously. Equations (17)-(18) specify the spatial evolution of the wave function and equation (27) reflects the spatial extent of the self-field of the particle. A strategy for solving these intrinsically non-linear equations, as well as a few of their interesting properties, will be explored in the following sections.

## 4 Boundary Conditions

From the previous section we have found that the equations to be satisfied for a self-interacting fermion are equations (17)-(18) and

$$\nabla^2 V = -4\pi e^2 \frac{2(l-j)}{2l+1} (f^2 + g^2) \left[ (\kappa + m + 1) |Y_l^{m+1}(\theta, \varphi)|^2 + (\kappa - m) |Y_l^m(\theta, \varphi)|^2 \right] \quad (28)$$

where we have combined the  $j = l \pm 1/2$  cases by using the definition of  $\kappa$ . Since we have assumed that the potential  $V$  in equations (17)-(18) is spherically symmetric, this necessarily restricts the choice of  $l$  and  $m$ . Assume from this point on that  $l$  and  $m$  are chosen to satisfy this criterion. Consequently, equation (28) becomes

$$\nabla^2 V = -e^2 (f^2 + g^2). \quad (29)$$

Since the soliton aspires as a coupling between Dirac and Maxwell fields, the energy  $E$  that appears in the Dirac equation is not the total energy of the particle. The total energy can be obtained by calculating the  $T_0^0$  component of the energy-momentum tensor. For our field, the Lagrangian is given by equation (1) where  $A^\mu$  is the vector potential of the electromagnetic field. One generates the symmetric energy-momentum tensor directly from the Lagrangian in the form[14]

$$T^{\mu\nu} = \frac{\partial L}{\partial g_{\mu\nu}} - \frac{g^{\mu\nu}}{2} L. \quad (30)$$

Applying (30) to (1) yields

$$\begin{aligned} T^{\mu\nu} = & \left[ \frac{i\hbar c}{2} (\bar{\psi}\gamma^\mu\partial^\nu\psi + \bar{\psi}\gamma^\nu\partial_\mu\psi) - \frac{1}{4\pi} F^{\alpha\mu} F^{\beta\nu} g_{\alpha\beta} - \frac{e}{2} (\bar{\psi}\gamma^\mu\psi A^\nu + \bar{\psi}\gamma^\nu\psi A^\mu) \right] \\ & - \frac{g^{\mu\nu}}{2} \left[ i\hbar c \bar{\psi}\gamma^\alpha g_{\alpha\beta} \partial^\beta\psi - mc^2 \bar{\psi}\psi - \frac{1}{8\pi} F^{\alpha\beta} F_{\alpha\beta} - e\bar{\psi}\gamma^\alpha\psi A^\beta g_{\alpha\beta} \right]. \end{aligned}$$



Further simplification gives

$$T_0^0 = E\psi^\dagger\psi + \frac{1}{8\pi} \left( \frac{d\phi}{dr} \right)^2.$$

This yields an expression for the total energy,  $E_{\text{tot}}$ , of

$$\begin{aligned} E_{\text{tot}} &= \int T_0^0 dV_{ol} \\ &= E \int_0^\infty (f^2 + g^2) r^2 dr + \frac{1}{2} \int \left( \frac{d\phi}{dr} \right)^2 r^2 dr \end{aligned} \quad (31)$$

where  $dV_{ol}$  is an infinitesimal volume element. This total energy should be associated with the observed mass of the particle as  $E_{\text{tot}} = mc^2$ . There is still sufficient freedom remaining to set  $\lim_{r \rightarrow \infty} V(r) = 0$  because the spinor is invariant under the transformation

$$V \rightarrow V + \beta; \quad E \rightarrow E + \beta$$

for any real-valued  $\beta$ .

The mass  $m$  and the charge  $e$  that appear in the Dirac equation are not necessarily the experimentally measured quantities just as the charge that appears at a vertex of a Feynman graph is not the experimentally measured charge of the particle. Because of this, we will replace the  $m$  in (17)-(18) by the symbol  $\mu$ . In addition, the  $e$  in (29) will be replaced by an  $\epsilon$ . The symbols  $m$  and  $e$  will be reserved for the physically observed quantities. With these substitutions, we convert to a set of variables whereby equations (17), (18) and (31) are independent of any physical constants. The particular transformation chosen is

$$f = \eta F, \quad g = \eta G, \quad r = \frac{\hbar x}{\mu c}, \quad E = \lambda \mu c^2, \quad V = \mu c^2 U$$

where  $\eta^2 = \mu^3 c^4 / \epsilon^2 \hbar^2$ . These redefined variables have the following dimensions in terms of length ( $L$ ):

$$[x] = L^0; \quad [\lambda] = L^0; \quad [F] = L^{-3/2}; \quad [G] = L^{-3/2}; \quad [U] = L^0.$$

This yields the transformed equations:

$$[\lambda - U(x) + 1] F(x) - \left[ \frac{dG}{dx} + \frac{1 + \kappa}{x} G(x) \right] = 0 \quad (32)$$

$$[\lambda - U(x) - 1] G(x) + \left[ \frac{dF}{dx} + \frac{1 - \kappa}{x} F(x) \right] = 0 \quad (33)$$

$$\nabla^2 U + (F^2 + G^2) = 0 \quad (34)$$

where  $\nabla^2$  is now the Laplacian with respect to the  $x$  coordinate. The mass of the soliton comes from the transformed version of the total energy expression (31),

$$mc^2 = \frac{\hbar \mu c^3}{\epsilon^2} \left[ \lambda \int_0^\infty (F^2 + G^2) x^2 dx + \frac{1}{2} \int_0^\infty \left( \frac{dU}{dx} \right)^2 x^2 dx \right] \quad (35)$$

and the total charge is given as the integral of the charge density

$$e = \epsilon \int \rho dV_{ol} = \frac{\hbar c}{\epsilon} \int_0^\infty (F^2 + G^2) x^2 dx. \quad (36)$$

We will show that if the charge  $\epsilon$  is replaced by  $e$ , that the  $f$  component of the spinor greatly dominates the  $g$  component. By substituting  $\epsilon = e$  and choosing a value for  $m$ , the value of  $\mu$  can be determined numerically once the spatial extent of the soliton is known. In this case, the expectation value of the radius of the particle becomes

$$\langle r \rangle = \frac{\hbar c}{\mu c^2} \langle x \rangle = \frac{e^2 \hbar c}{\mu c^2 e^2} \frac{\int \nabla^2 U x^3 dx}{\int \nabla^2 U x^2 dx} = \frac{e^2}{\mu c^2} \frac{\int \nabla^2 U x^3 dx}{\left[ \int \nabla^2 U x^2 dx \right]^2}.$$

To stay within the current experimental bounds of the mean charge radius, this value must be less than  $r_{exp}$  which is  $\leq 10^{-18}m$  in the case of an electron. Hence,

$$\int_0^\infty \nabla^2 U x^3 dx \leq \frac{r_{exp} \mu}{r_e m_e} \left[ \int_0^\infty \nabla^2 U x^2 dx \right]^2$$

where  $r_e$  is the classical electron radius  $r_e = e^2/m_e c^2$ .

Since we know that  $U$  has zero slope at  $x = 0$  and that it must behave as  $N/x$  for large argument ( $N$  is the amount of enclosed charge), we assume as a first approximation, that  $U$  can be represented as the electrostatic potential produced by a sphere of radius  $R_0$  with uniform charge density. Therefore,

$$U(r) = \begin{cases} \frac{N}{R_0} \left[ \frac{3}{2} - \frac{1}{2} \frac{r^2}{R_0^2} \right] & \text{for } r < R_0 \\ \frac{N}{r} & \text{for } r \geq R_0. \end{cases} \quad (37)$$

With this representation, one finds that

$$\langle r \rangle = \frac{9 r_e m_e R_0}{4 \mu N}$$

which means that since  $0 < \langle r \rangle < r_{exp}$ , we can conclude that

$$0 < \frac{R_0}{\mu N} < \frac{4 r_{exp}}{9 r_e m_e} \simeq 3.088 \times 10^{-4} c^2/\text{MeV}$$

in the case of the electron.

Let  $R_0$  be defined as the effective range of the non-Coulombic behaviour of the potential energy so that for  $x > R_0$ ,  $U(x) \sim N/x$ . Since  $U$  is a solution to a Poisson equation with

a negative definite charge density,  $U(0)$  must be larger than  $U(R_0)$ . This can be quickly verified by considering the opposite. If  $U(0) < U(R_0)$  then there exists some  $r \in (0, R_0)$  such that  $U'(r) = 0$ . Therefore integrating (34) from 0 to  $r$ , one obtains

$$r^2 U'(r) = 0 = - \int_0^r (F^2 + G^2) x^2 dx$$

which is clearly a contradiction.

To determine the initial values of  $F$  and  $G$ , one simply eliminates either  $F$  or  $G$  from (32-33), say  $F$ , which leads to a second order equation for the other, namely,

$$G'' + PG' + QG = 0$$

where both  $P$  and  $Q$  are functions of  $U$ ,  $U'$ ,  $\kappa$ ,  $\lambda$  and  $x$ . To avoid a singularity in the potential  $U(x)$ , it must be both bounded and have zero slope in a neighbourhood of the origin. Moreover, both  $F$  and  $G$  are bounded in this same neighbourhood. From this, it is easy to verify that

$$F(0) = \begin{cases} 0 & \kappa = -1 \\ \text{arbitrary} & \kappa = +1 \\ 0 & \forall \text{ other } \kappa, \end{cases} \quad (38)$$

$$G(0) = \begin{cases} \text{arbitrary} & \kappa = -1 \\ 0 & \kappa = +1 \\ 0 & \forall \text{ other } \kappa. \end{cases} \quad (39)$$

Furthermore, by examining the indicial equation, it can be shown that no fractional powers exist in a power series solution of either  $F$  or  $G$  about the origin  $x = 0$ .

Summarizing the boundary conditions:

$$U(x) < U(0) < \infty, \quad x \in [0, \infty), \\ U'(0) = 0,$$

together with the conditions (38), (39). For the case  $\kappa = -1$ , the initial values of  $U$ ,  $G$  and the energy  $\lambda$  are determined by the requirement that the wave function  $\psi$ , and hence both  $F$  and  $G$ , vanish exponentially as  $x \rightarrow \infty$ .

## 5 Results

In the search for numerical solutions it was specified that  $\kappa = -1$  and  $\lambda = 1$  giving the set of differential equations

$$\begin{aligned} \frac{dG}{dx} &= [2 - U(x)] F(x) \\ \frac{dF}{dx} &= -\frac{2}{x} F(x) + U(x) G(x) \\ \nabla^2 U &= -F^2 - G^2. \end{aligned}$$

To find a soliton, the values of  $F(0)$ ,  $G(0)$  are specified and a search is made for the value of  $U(0)$  whereby  $\lim_{x \rightarrow \infty} xF(x) = 0$  and  $\lim_{x \rightarrow \infty} xG(x) = 0$ . Only values of  $G(0) > 0$  are considered because the equations are symmetric under the transformation  $G \rightarrow -G$ ,  $F \rightarrow -F$ ,  $U \rightarrow U$ . In a neighbourhood of a ground state soliton, the radial probability density is numerically seen to have a single well-defined minimum value for  $x > 0$ . The choice of  $\kappa = -1$  gives the initial condition  $F(0) = 0$ .

The choice of  $\lambda = 1$  is simply a numerical convenience. Outside the neighbourhood of a soliton it is expected that the potential will behave as  $U(x) \sim A + B/x$  for large  $x$ . The value of  $\lambda$  should have been chosen so that the asymptotic behaviour of the potential  $U(x)$  is purely Coulombic in nature. By defining a shifted potential  $\tilde{U}(x) = U(x) - \lim_{x \rightarrow \infty} U(x)$ , this value of  $\lambda$  must satisfy  $1 - U(x) = \lambda - \tilde{U}(x)$ . Therefore after a soliton is found the value of  $\lambda$  is given as  $\lambda = 1 - \lim_{x \rightarrow \infty} U(x)$ . In addition, the starting value of  $\tilde{U}(x)$  is given by  $\tilde{U}(0) = U(0) + \lambda - 1$ .

Using the redefined value of  $\lambda$  the observed charge and mass of the particle are compared to the values used in the Lagrangian by using the expressions (36) and (35) respectively. By defining

$$\mathcal{P} = \int_0^\infty (F^2 + G^2) x^2 dx, \quad \mathcal{X} = \int_0^\infty (F^2 + G^2) x^3 dx,$$

$$\mathcal{E} = \lambda \mathcal{P} + \frac{1}{2} \int_0^\infty \left( \frac{dU}{dx} \right)^2 x^2 dx,$$

the charge ratio  $\epsilon/e$  is given as

$$\frac{\epsilon}{e} = \frac{\hbar c}{e^2} \mathcal{P} = \frac{\mathcal{P}}{\alpha}$$

where  $\alpha$  is the fine structure constant. The mass ratio  $\mu/m = \mathcal{P}^2/\alpha \mathcal{E}$  and the expectation value for the radius of the soliton is

$$\langle r \rangle = \frac{\int (f^2 + g^2) r^3 dr}{\int (f^2 + g^2) r^2 dr} = \frac{\hbar}{\mu c} \frac{\int (F^2 + G^2) x^3 dx}{\int (F^2 + G^2) x^2 dx} = r_e \left( \frac{m_e}{m} \right) \frac{\mathcal{E} \mathcal{X}}{\mathcal{P}^3}.$$

Both of the quantities  $\mathcal{P}$  and  $\mathcal{X}$  are positive. However, depending upon the value of  $\lambda$ ,  $\mathcal{E}$  could be positive, negative or even zero if the electromagnetic and “bare mass” terms in the energy exactly cancel. A negative value for  $\mathcal{E}$  will give an unphysical negative value for the observed radius  $\langle r \rangle$ . Because of this ambiguity, both the value of  $\langle r \rangle$  and the particle width  $\Delta r = \sqrt{\langle r^2 \rangle - \langle r \rangle^2}$  are presented. Tables 2 and 3 respectively list the numerical parameters and the observed properties of a number of ground state particles found where  $m$  was taken to be the observed mass of the electron  $m_e$ .

Figure 1 illustrates the radial behaviour of  $F$  and  $G$  for the case  $\epsilon = e$  ( $i = 1$ ). It is to be noted that for  $x > 0$ ,  $F$  is much larger than  $G$  and as a consequence,  $FG \ll F^2 + G^2$ . In fact,  $G$  is so small that it resembles a straight line along the  $x$  axis. This supports the argument that the four-vector potential can be reasonably approximated with only a radial  $A^0$  component.

The characteristics of a typical soliton with  $\epsilon \neq e$  is illustrated with the choice  $\epsilon/e = 454.8$  ( $i = 19$ ). In this case the potential plays a much more dominant role in holding the particle together than in the case  $\epsilon = e$ . However, since in this case the approximation of  $FG \ll F^2 + G^2$  is violated, one would have to solve the full model (equations (9)-(10)) to properly analyse this situation. This would be a far more complicated problem. Figure 2 illustrates the radial components of this spinor and it shows that the magnitude of  $G$  is now comparable to the magnitude of  $F$ . Table 3 also shows that the choice of  $\epsilon = 389.0e$ ,  $\mu = 2.360 \times 10^{12}m_e$  ( $i = 15$ ) yields a soliton with an expectation value for the radius of  $5.05 \times 10^{-23}m$ . This size is well within the present experimentally determined upper limit for the electron radius of  $\simeq 10^{-18}m$ .

These equations also exhibit excited states. The  $n^{\text{th}}$  excited state of our field is characterized through the functions  $F_n(x)$ ,  $G_n(x)$  and  $U_n(x)$  for which the  $G_n$  component crosses the abscissa  $n + 1$  times while the  $F_n$  component crosses it  $n$  times. Once the ground state solution is found, the value of  $\mu$  can be determined through equation (36). The corresponding  $n^{\text{th}}$  excited state is that excited state with the same observed charge ratio,  $\epsilon/e$ , as the ground state. Therefore, in this interpretation of the theory, the ratio of the mass of the  $n^{\text{th}}$  excited state to the ground state is given by the expression

$$\frac{m_n}{m_0} = \frac{\mu/m_0}{\mu/m_n} = \frac{\lambda_n \int_0^\infty (F_n^2 + G_n^2) x^2 dx + \frac{1}{2} \int_0^\infty \left(\frac{dU_n}{dx}\right)^2 x^2 dx}{\lambda \int_0^\infty (F^2 + G^2) x^2 dx + \frac{1}{2} \int_0^\infty \left(\frac{dU}{dx}\right)^2 x^2 dx}.$$

Figure 3 shows radial probability density of the first three states for the case  $G(0) = 1$ . Each of these solitons has a different value of  $\epsilon/e$ .

Figure 4 illustrates the behaviour of the mass ratio,  $\mu/m$ , as a function of the charge ratio  $\epsilon/e$  for the ground state and the first two excited states. For each class of particles there is a charge ratio where the electromagnetic and bare mass components of the energy balance making  $\mathcal{E} = 0$ . At this value of  $\epsilon/e$ , the mass ratio  $\mu/m \rightarrow \infty$ . At charge ratios less than this critical value the mass ratio is negative whereas charge ratios above this critical value result in a positive value of  $\mu/m$ . There is numerical evidence that each class of particles has an upper bound for the charge ratio. Above this maximum charge ratio we were unable to find any solutions such that  $\lim_{x \rightarrow \infty} xF(x) \rightarrow 0$  or  $\lim_{x \rightarrow \infty} xG(x) \rightarrow 0$ . This necessarily restricts the definition of the mass ratio defined above. Figure 4 also illustrates the fact that at moderate charge ratios, the electromagnetic field does not contain an appreciable amount of the particle energy resulting in the behaviour  $|\mu/m| \simeq \epsilon/e$ .

The mass ratios of the first and second excited states with respect to the ground state solutions are shown in figure 5. This ratio is only defined up to a maximum value of  $\epsilon/e$  since beyond  $\epsilon/e \simeq 550$ , a ground state fails to exist. For excited states, this maximum admissible charge ratio increases. This implies that for a fixed value of  $\epsilon/e$  there may not exist a ground state solution, but there will be arbitrarily many excited states. As is readily apparent from

figure 5, the only appreciable mass splitting occurs for large charge ratios. However, it is precisely for large charge ratios where our approximation that  $FG \ll F^2 + G^2$  breaks down.

## 6 Concluding Remarks

We have seen that spherically symmetric Dirac-Maxwell solitons can be constructed and with a charge and mass to model the electron successfully. However, it should be noted that the higher energy excited states of this form did not yield the large mass separations of the muon and tau relative to the electron in this model. The search thus far has been restricted to spherical solitons. It is conceivable that a relaxation of this restriction or some other change in conditions would increase the mass splitting. In any event, we have shown that Dirac-Maxwell solitons exist and are capable of modelling an electron where the charge-to-mass ratio is the observed  $\simeq 10^{21}$  in units in which  $G = c = 1$ . Furthermore, we have found a charge-to-mass ratio that simultaneously yields the observed charge and mass of the electron as well as exhibiting a degree of compactification that is well within the current experimental upper limit. Finster et al.[8] have considered Einstein-Dirac-Maxwell (EDM) solitons and concluded that it is the interaction with gravitation which is responsible for the existence of bound states. However, we see here that bound states exist with negligible gravitational interaction. While the  $e/m$  ratio at which significant gravitational coupling sets in is yet to be determined for EDM solitons, it is our conjecture that this will be so at the same level that was found earlier in the case of minimally coupled scalar interaction[4], namely for  $e/m \simeq 1$ . The known fundamental charged particles of nature, on the other hand have enormous  $e/m$  ratios.

## REFERENCES

- [1] Einstein, A. & Rosen, N. (1935). *Physical Review*, **48**, 73-77.
- [2] Rosen, N. (1939). *Physical Review*, **55**, 94-101.
- [3] Rosen, N. & Rosenstock, H. B. (1952). *Physical Review*, **85**(2), 257-259.
- [4] Cooperstock, F. I. & Rosen, N. (1989). *International Journal of Theoretical Physics*, **28**(4), 423-440.
- [5] Cooperstock, F. I. (1991). *The Electron: New Theory and Experiment*, Eds. D. Hestenes and A. Weingartshofer, Kluwer Academic.
- [6] Bohun, C. S. (1991). *A Self-Consistent Dirac-Maxwell Field of Solitons*, MSc. Thesis, University of Victoria.

- [7] Lisi, A. G. (1995). *Journal of Physics A: Mathematical and General*, **28**, 5385-5392.
- [8] Finster, F., Smoller, J. and Yau, S-T., preprint gr-qc/9801079
- [9] Griffiths, D. J. (1987). *Introduction to Elementary Particles*. New York: Harper and Row.
- [10] Bethe, H. A. & Salpeter, E. E. (1957). *Quantum Mechanics of One- and Two- Electron Atoms*. Berlin: Springer-Verlag.
- [11] Evans, L. C. (1998). *Partial Differential Equations: Graduate Studies in Mathematics, vol 19*. American Mathematical Society, Providence, Rhode Island. p. 22.
- [12] Brezzi, F. & Markowich, P. A. (1991). *Mathematical Methods in the Applied Sciences*, **14**, 35-61.
- [13] Abramowitz, M & Stegun, I. A. (1964). *Handbook of mathematical functions, with formulas, graphs, and mathematical tables*. National Bureau of Standards, United States Department of Commerce.
- [14] Landau, L. D. & Lifshitz E. M. (1971). *The classical theory of fields* (4th ed.). New York: Pergamon Press.

## A Derivatives of $f(r)Y_l^m(\theta, \varphi)$

In the Dirac wave equation, all of the derivatives are with respect to Cartesian coordinates. We can change to a spherical polar representation via the transformation

$$\begin{aligned}x &= r \sin \theta \cos \varphi \\y &= r \sin \theta \sin \varphi \\z &= r \cos \theta.\end{aligned}$$

By applying the chain rule, it is trivial to show that this changes the first order partial derivatives via

$$\frac{\partial}{\partial x} = \sin \theta \cos \varphi \frac{\partial}{\partial r} + \frac{\cos \theta \cos \varphi}{r} \frac{\partial}{\partial \theta} - \frac{\sin \varphi}{r \sin \theta} \frac{\partial}{\partial \varphi} \quad (\text{A.1})$$

$$\frac{\partial}{\partial y} = \sin \theta \sin \varphi \frac{\partial}{\partial r} + \frac{\cos \theta \sin \varphi}{r} \frac{\partial}{\partial \theta} + \frac{\cos \varphi}{r \sin \theta} \frac{\partial}{\partial \varphi} \quad (\text{A.2})$$

$$\frac{\partial}{\partial z} = \cos \theta \frac{\partial}{\partial r} - \frac{\sin \theta}{r} \frac{\partial}{\partial \theta}. \quad (\text{A.3})$$

If the functions  $\psi_j (j = 1, \dots, 4)$  from expression (7) are substituted into (13)-(16), and if one uses the formulas given in Bethe and Salpeter[10] for the derivatives of a function of the

form  $f(r)Y_l^m(\theta, \varphi)$  with respect to  $x$ ,  $y$ , and  $z$ , one finds a coupled pair of first order ordinary equations for  $f(r)$  and  $g(r)$ .

For example, in order to calculate

$$\frac{\partial}{\partial z} [f(r)Y_l^m(\theta, \varphi)],$$

we first require the identities

$$\cos \theta P_l^m(\cos \theta) = \frac{1}{2l+1} [(l-m+1)P_{l+1}^m(\cos \theta) + (l+m)P_{l-1}^m(\cos \theta)] \quad (\text{A.4})$$

$$\sin \theta \frac{d}{d\theta} P_l^m(\cos \theta) = \frac{1}{2l+1} [l(l-m+1)P_{l+1}^m(\cos \theta) - (l+1)(l+m)P_{l-1}^m(\cos \theta)], \quad (\text{A.5})$$

which can both be verified through the use of Rodrigues' formula

$$P_l^m(\mu) = \frac{(-1)^m}{2^l l!} (1-\mu^2)^{m/2} \frac{d^{l+m}}{d\mu^{l+m}} (\mu^2-1)^l.$$

Writing  $Y_l^m(\theta, \varphi)$  as a function of  $P_l^m$  by using (8) gives the relationship

$$\frac{\partial}{\partial z} [f(r)Y_l^m(\theta, \varphi)] = \sqrt{\frac{2l+1}{4\pi} \frac{(l-m)!}{(l+m)!}} e^{im\varphi} \left[ \cos \theta P_l^m(\cos \theta) \frac{df}{dr} - \sin \theta \frac{d}{d\theta} P_l^m(\cos \theta) \frac{f}{r} \right].$$

By substituting (A.4-A.5) in the above, collecting terms, and applying the definition of  $Y_l^m(\theta, \varphi)$  once again, one obtains the simplification

$$\begin{aligned} \frac{\partial}{\partial z} [f(r)Y_l^m(\theta, \varphi)] &= \sqrt{\frac{(l-m+1)(l+m+1)}{(2l+1)(2l+3)}} Y_{l+1}^m(\theta, \varphi) \left[ \frac{df}{dr} - \frac{l}{r} f \right] \\ &+ \sqrt{\frac{(l-m)(l+m)}{(2l-1)(2l+1)}} Y_{l-1}^m(\theta, \varphi) \left[ \frac{df}{dr} + \frac{l+1}{r} f \right]. \end{aligned} \quad (\text{A.6})$$

Similar relationships for  $\frac{\partial}{\partial x} \pm i \frac{\partial}{\partial y}$  can be found in Bethe and Salpeter<sup>3</sup>, but there is a very elegant way to derive these operators by applying the Wigner-Eckart theorem.

First, we evaluate the matrix element  $\langle l 0 | \nabla_0 | l 0 \rangle$  of the gradient operator, which is an example of a vector operator. Specifically,

$$\nabla_0 = \frac{\partial}{\partial z}, \quad \nabla_{\pm} = \mp \frac{1}{\sqrt{2}} \left( \frac{\partial}{\partial x} \pm i \frac{\partial}{\partial y} \right).$$

Since

$$\nabla_0 f(r)Y_l^0 = \frac{l+1}{\sqrt{(2l+1)(2l+3)}} Y_{l+1}^0 \left[ \frac{df}{dr} - \frac{l}{r} f \right] + \frac{l}{\sqrt{(2l-1)(2l+1)}} Y_{l-1}^0 \left[ \frac{df}{dr} + \frac{l+1}{r} f \right]$$

<sup>3</sup>See formula (A.38) and (A.39) respectively in Bethe and Salpeter.



for the special case of (A.6) where  $m = 0$ , we have

$$\langle l' 0 | \nabla_0 | l 0 \rangle = \frac{l+1}{\sqrt{(2l+1)(2l+3)}} \left[ \frac{df}{dr} - \frac{l}{r} f \right] \delta_{l'+1}^{l'} + \frac{l}{\sqrt{(2l-1)(2l+1)}} \left[ \frac{df}{dr} + \frac{l+1}{r} f \right] \delta_{l-1}^{l'}.$$

Now, we are at a point where we can use the Wigner–Eckart theorem. By inspection, the general matrix element is given by

$$\begin{aligned} \langle l' m' | \nabla_\mu | l m \rangle &= (-1)^{l'-m'} \begin{pmatrix} l' & 1 & l \\ -m' & \mu & m \end{pmatrix} \langle l' || \nabla || l \rangle \\ &= (-1)^{m'} \frac{\begin{pmatrix} l' & 1 & l \\ -m' & \mu & m \end{pmatrix}}{\begin{pmatrix} l' & 1 & l \\ 0 & 0 & 0 \end{pmatrix}} \langle l' 0 | \nabla_0 | l 0 \rangle. \end{aligned}$$

After evaluating the  $3-j$  symbols, one can quickly verify the following equations.

$$\begin{aligned} \frac{\partial}{\partial z} [f(r) Y_l^m(\theta, \varphi)] &= \sqrt{\frac{(l-m+1)(l+m+1)}{(2l+1)(2l+3)}} Y_{l+1}^m(\theta, \varphi) \left[ \frac{df}{dr} - \frac{l}{r} f \right] \\ &+ \sqrt{\frac{(l-m)(l+m)}{(2l-1)(2l+1)}} Y_{l-1}^m(\theta, \varphi) \left[ \frac{df}{dr} + \frac{l+1}{r} f \right] \end{aligned} \quad (\text{A.7})$$

$$\begin{aligned} \left[ \frac{\partial}{\partial x} + i \frac{\partial}{\partial y} \right] [f(r) Y_l^m(\theta, \varphi)] &= \sqrt{\frac{(l+m+1)(l+m+2)}{(2l+1)(2l+3)}} Y_{l+1}^{m+1}(\theta, \varphi) \left[ \frac{df}{dr} - \frac{l}{r} f \right] \\ &- \sqrt{\frac{(l-m-1)(l-m)}{(2l-1)(2l+1)}} Y_{l-1}^{m+1}(\theta, \varphi) \left[ \frac{df}{dr} + \frac{l+1}{r} f \right] \end{aligned} \quad (\text{A.8})$$

$$\begin{aligned} \left[ \frac{\partial}{\partial x} - i \frac{\partial}{\partial y} \right] [f(r) Y_l^m(\theta, \varphi)] &= -\sqrt{\frac{(l-m+1)(l-m+2)}{(2l+1)(2l+3)}} Y_{l+1}^{m-1}(\theta, \varphi) \left[ \frac{df}{dr} - \frac{l}{r} f \right] \\ &+ \sqrt{\frac{(l+m-1)(l+m)}{(2l-1)(2l+1)}} Y_{l-1}^{m-1}(\theta, \varphi) \left[ \frac{df}{dr} + \frac{l+1}{r} f \right]. \end{aligned} \quad (\text{A.9})$$

Linear combinations of (A.8) and (A.9) yield the derivatives with respect to  $x$  and  $y$ .

States $ l', m', j'\rangle$	Corresponding Potential $V(\mathbf{r})$
$ 0, 0, 1/2\rangle,  0, -1, 1/2\rangle$	$e^2 I_0$
$ 1, 0, 1/2\rangle,  1, -1, 1/2\rangle$	$e^2 I_0$
$ 1, 1, 3/2\rangle,  0, -2, 3/2\rangle$	$e^2 \left[ I_0 - \frac{3}{2} (3 \cos^2 \theta' - 1) I_2 \right]$
$ 1, 0, 3/2\rangle,  0, -1, 3/2\rangle$	$e^2 \left[ I_0 + \frac{3}{2} (3 \cos^2 \theta' - 1) I_2 \right]$

Table 1: The Dirac–Maxwell particle self-field potential.

The self-field potential energy for a Dirac–Maxwell particle in the states  $l = 0, 1$  where

$$I_l(r) = \int_0^r [f(r')^2 + g(r')^2] \frac{r'^{l+2}}{r^{l+1}} dr' + \int_r^\infty [f(r')^2 + g(r')^2] \frac{r^l}{r'^{l-2}} dr'.$$


---

$i$	$G(0)$	$U(0)$	$\lambda$	$x_{\max}$
1	$3.864 \times 10^{-9}$	$4.8879852 \times 10^{-6}$	-0.99999712	8342.9
2	$1.0 \times 10^{-8}$	$9.2122047 \times 10^{-6}$	-0.99999457	6103.6
3	$1.0 \times 10^{-5}$	$9.2122842 \times 10^{-4}$	-0.99945701	688.37
4	$1.0 \times 10^{-4}$	$4.2760987 \times 10^{-3}$	-0.99748078	330.61
5	$1.0 \times 10^{-3}$	$1.9850763 \times 10^{-2}$	-0.98833078	158.92
6	$5.0 \times 10^{-3}$	$5.8063758 \times 10^{-2}$	-0.96604870	81.570
7	$1.0 \times 10^{-2}$	$9.2196988 \times 10^{-2}$	-0.94634242	77.061
8	$5.0 \times 10^{-2}$	$2.6992683 \times 10^{-1}$	-0.84654287	50.139
9	$1.0 \times 10^{-1}$	$4.2884212 \times 10^{-1}$	-0.76093227	38.686
10	$2.0 \times 10^{-1}$	$6.8134130 \times 10^{-1}$	-0.63095887	33.509
11	$3.0 \times 10^{-1}$	$8.9315883 \times 10^{-1}$	-0.52683528	23.495
12	$4.0 \times 10^{-1}$	$1.0821393 \times 10^0$	-0.43716613	26.964
13	$4.1 \times 10^{-1}$	$1.1001061 \times 10^0$	-0.42878460	27.544
14	$4.2 \times 10^{-1}$	$1.1179261 \times 10^0$	-0.42049493	26.049
15	$G^*(0)$	$1.1309487 \times 10^0$	-0.41445154	24.146
16	$4.3 \times 10^{-1}$	$1.1356039 \times 10^0$	-0.41229414	24.382
17	$5.0 \times 10^{-1}$	$1.2557044 \times 10^0$	-0.35715757	24.156
18	$6.0 \times 10^{-1}$	$1.4178526 \times 10^0$	-0.28421512	22.584
19	$1.0 \times 10^0$	$1.9913670 \times 10^0$	-0.03776277	20.438
20	$2.0 \times 10^0$	$3.1519761 \times 10^0$	+0.42244841	18.125

Table 2: Numerical parameters for a set of various ground state particles. For each particle, the value of  $G(0)$  is selected and one searches for the value of  $U(0) + \lambda$  that gives a bounded solution. The physical parameters are computed from the solution defined on  $x \in [0, x_{\max}]$ .  $G^*(0) = 0.4273589430$ .

---

$i$	$\epsilon/e$	$\mu/m$	$\langle r \rangle$	$\Delta r$
1	1.000	$-1.000 \times 10^0$	$-6.61 \times 10^{-8}$	$2.31 \times 10^{-8}$
2	1.371	$-1.371 \times 10^0$	$-3.51 \times 10^{-8}$	$1.22 \times 10^{-8}$
3	13.74	$-1.374 \times 10^1$	$-3.51 \times 10^{-10}$	$1.22 \times 10^{-10}$
4	29.55	$-2.955 \times 10^1$	$-7.53 \times 10^{-11}$	$2.63 \times 10^{-11}$
5	63.46	$-6.462 \times 10^1$	$-1.60 \times 10^{-11}$	$5.61 \times 10^{-12}$
6	107.6	$-1.135 \times 10^2$	$-5.30 \times 10^{-12}$	$1.87 \times 10^{-12}$
7	134.7	$-1.479 \times 10^2$	$-3.21 \times 10^{-12}$	$1.14 \times 10^{-12}$
8	222.1	$-2.991 \times 10^2$	$-9.07 \times 10^{-13}$	$3.31 \times 10^{-13}$
9	271.3	$-4.504 \times 10^2$	$-4.64 \times 10^{-13}$	$1.73 \times 10^{-13}$
10	326.2	$-8.687 \times 10^2$	$-1.87 \times 10^{-13}$	$7.23 \times 10^{-14}$
11	359.7	$-1.838 \times 10^3$	$-7.51 \times 10^{-14}$	$2.99 \times 10^{-14}$
12	383.6	$-9.658 \times 10^3$	$-1.27 \times 10^{-14}$	$5.16 \times 10^{-15}$
13	385.6	$-1.538 \times 10^4$	$-7.89 \times 10^{-15}$	$3.21 \times 10^{-15}$
14	387.6	$-3.666 \times 10^4$	$-3.28 \times 10^{-15}$	$1.34 \times 10^{-15}$
15	389.0	$+2.360 \times 10^{12}$	$+5.05 \times 10^{-23}$	$2.06 \times 10^{-23}$
16	389.5	$+1.032 \times 10^5$	$+1.15 \times 10^{-15}$	$4.71 \times 10^{-16}$
17	401.8	$+3.998 \times 10^3$	$+2.79 \times 10^{-14}$	$1.16 \times 10^{-14}$
18	416.4	$+1.818 \times 10^3$	$+5.68 \times 10^{-14}$	$2.39 \times 10^{-14}$
19	454.8	$+6.800 \times 10^2$	$+1.21 \times 10^{-13}$	$5.35 \times 10^{-14}$
20	498.7	$+3.305 \times 10^2$	$+1.78 \times 10^{-13}$	$8.59 \times 10^{-14}$

Table 3: Corresponding observable quantities for a set of various ground state particles. The values  $\langle r \rangle$  and  $\Delta r$  are measured in meters and are computed from a soliton defined on  $x \in [0, x_{\max}]$ . For this calculation it is assumed that  $m = m_e$ .

---

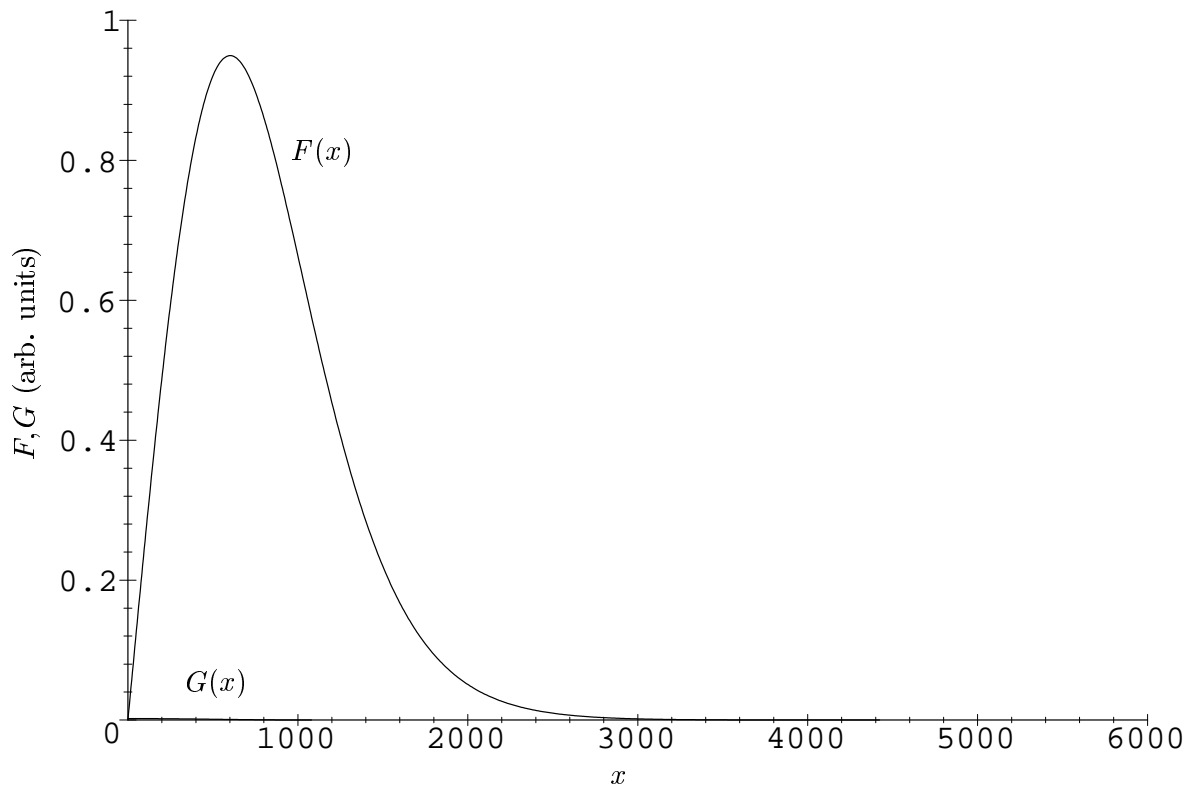


Figure 1:  $F$  and  $G$  components of the wave function for the case  $\epsilon/e = 1$ .  
 Shown here is the radial dependence of the  $F$  and  $G$  components of the soliton. Note that  $G$  is much smaller than  $F$ .  $G$  is barely discernible above the  $x$  axis.

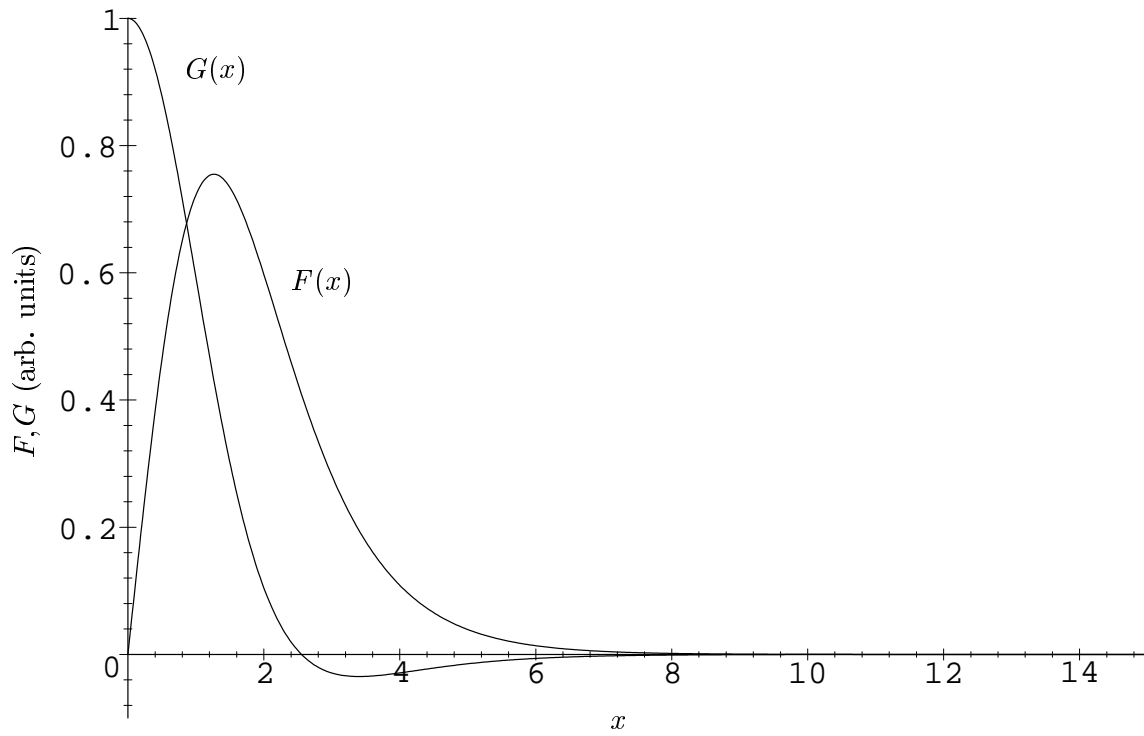


Figure 2:  $F$  and  $G$  components of the wave function for the case  $\epsilon/e = 454.8$ .

*Shown here is the radial dependence of the  $F$  and  $G$  components of the soliton. The magnitudes of  $F$  and  $G$  are now comparable in contrast to the case when  $\epsilon = e$ .*

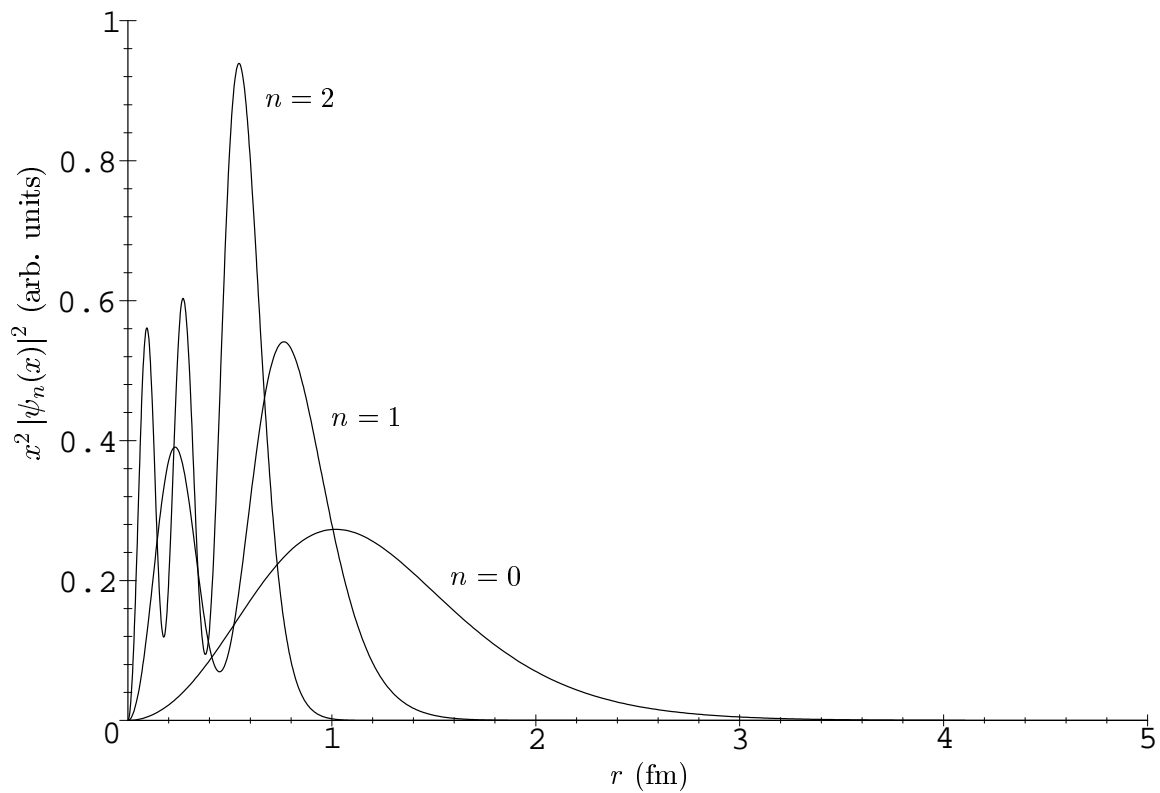


Figure 3: Excited states of the theory.

*This figure shows the radial probability density of the first three particle state in the case  $G(0) = 1$ . These particles have different charge ratios  $\epsilon/e$ . There exist excited states beyond the ones illustrated.*

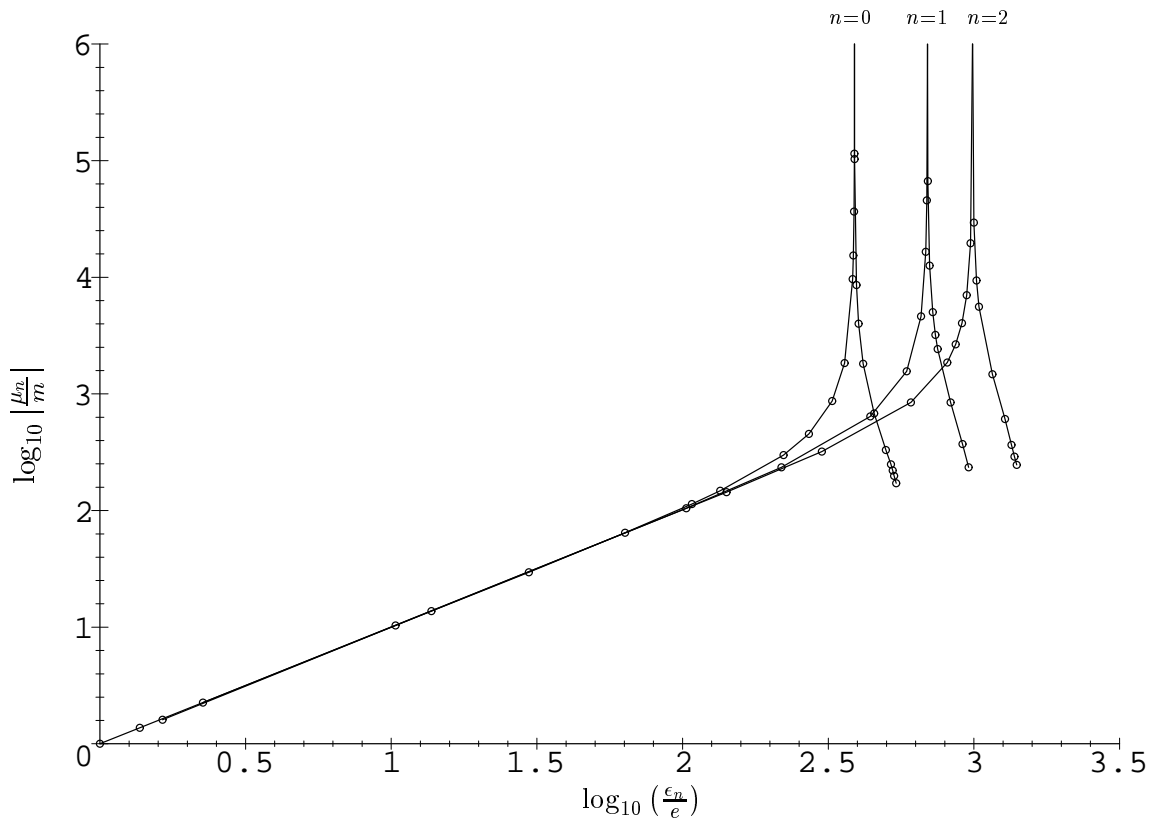


Figure 4: Dependence of the mass ratio as a function of the charge ratio.

*Shown is the dependence of the mass ratio  $\mu/m$  as a function of the charge ratio  $\epsilon/e$  for the ground state and first two excited state solitons. For each class of particles, there is a maximum charge ratio beyond which no solitons were found.*



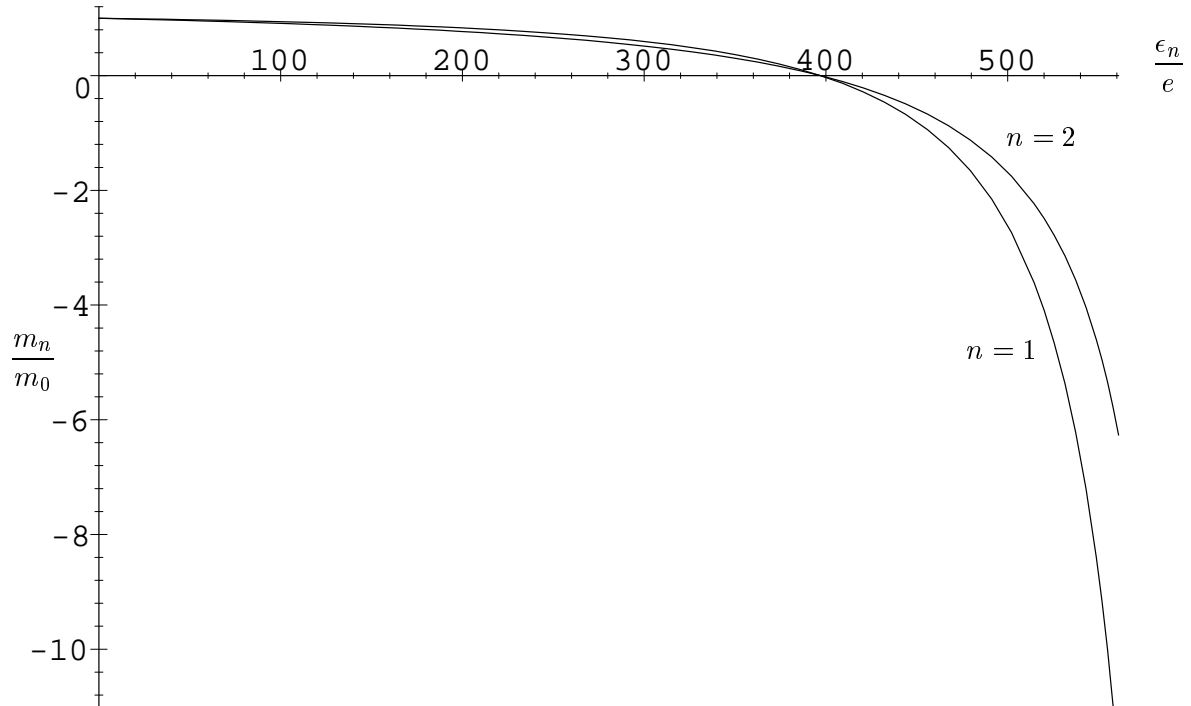


Figure 5: Mass ratios of the first and second excited states with respect to the ground state.

*There are essentially two regions of interest. For moderate charge ratios, the value of  $m_n/m_0 \simeq 1$  with the mass ratio of the excited state  $n = 2$  slightly larger than for the  $n = 1$  state. Beyond the point where the ground state mass ratio becomes unbounded, the mass ratios begin to split. In this region, the  $|m_1/m_0|$  ratio exceeds the  $|m_2/m_0|$  ratio. In this region the approximation  $FG \ll F^2 + G^2$  is no longer valid.*